Journal of Microscopy, Vol. 237, Pt 3 2010, pp. 275–281
Received 17 September 2008; accepted 31 March 2009
doi: 10.1111/j.1365-2818.2009.03242.x

Electron microscopy investigations of V defects in multiple InGaN/GaN quantum wells and InGaN quantum dots

J.R. YANG*, W.C. LI*, H.L. TSAI*, J.T. HSU† & M. SHIOJIRI‡
**Institute of Materials Science and Engineering, National Taiwan University, Taipei, Taiwan, Republic of China*
†Industrial Technology Research Institute, Hsinchu, Taiwan, Republic of China
‡Professor Emeritus of Kyoto Institute of Technology, 1-297 Wakiyama, Kyoto 618-0091, Japan

Key words. Energy dispersive X-ray spectroscopy nanoanalysis, high-angular annular dark field scanning transmission electron microscopy, high-resolution transmission electron microscopy, InGaN-based light emitting diode, laser diode, multiple quantum wells, three-dimensional quantum dots.

Summary

The mechanism of high emission of InGaN-based multiple quantum wells, which exhibit exceptionally high light emission efficiency despite their high defect density, is still not fully understood. Here, we deal with this problem, showing the details of structure and formation of V defects in the multiple quantum wells and reviewing interpretations proposed so far. Then, we show a structural investigation of three-dimensional high-density quantum dots, fabricated instead of quantum wells in the active layer. The shape and size of the InGaN quantum dots and the SiN_x masks for the growth of the dots have been revealed using high-angle annular dark field scanning transmission electron microscopy, energy dispersive X-ray spectroscopy nanoanalysis and high-resolution transmission electron microscopy.

Introduction

InGaN-based GaN light emitting diodes and laser diodes (LDs) have been widely manufactured for over a range of visible and ultraviolet wavelengths. This is due to high emission efficiency from the active $In_xGa_{1-x}N$ layers in which quite a few threading dislocations (TDs) are involved (Nakamura *et al.*, 1998). However, the mechanism of high light emission is still not fully understood. The first part of this paper deals with defects in InGaN quantum wells (QWs) that are a key of this problem, reviewing some of significant papers including our electron microscopic observations.

As discussed later, it was believed that the carriers deeply localized in quantum dots (QDs) and hindered from migrating towards dislocations in QWs may cause the electroluminescence surprisingly unaffected by numerous dislocations (Gérard *et al.*, 1996). Therefore, the performance of LDs was expected to be much improved if the density of QDs would be made much higher than that of dislocations. The structures having three-dimensional QDs, instead of QWs in the active layer, have been designed (Daudin *et al.*, 1997; Hirayama *et al.*, 1998). Next, we report on our structural investigation of an ultra-high density InGaN QD device that was prepared on this trial basis.

Correspondence to: Prof. M. Shiojiri. Tel: +81 (0)75 956 8064; e-mail: shiojiri@pc4.so-net.ne.jp

Defects in InGaN QWs

Structure and formation mechanism of V defects

TDs, most of which form due to lattice mismatch between the substrate Al_2O_3 and the nucleation layer GaN, reach the InGaN/GaN multiple quantum well (MQW) active layer through underlying epilayers despite applying ingenious dislocation reduction techniques such as the epitaxial lateral over-growth (Usui *et al.*, 1997; Nam *et al.*, 1997) and the AlGaN/GaN strained-layer superlattice claddings (Nakamura *et al.*, 1998; Kozodoy *et al.*, 1999). It is still not fully understood why the InGaN-based devices have extraordinarily high emission efficiency in spite of the high density of TDs.

TDs were found to disrupt the InGaN layer and to originate the V defects or inverted hexagonal pyramid defects (Wu *et al.*, 1998; Chen *et al.*, 1998). The names originate from the fact that an empty V-pit in hexahedron cone shape, with six sidewalls on the $\{10\bar{1}1\}$ planes, is formed during the MQW growth (Chen *et al.*, 1998), and subsequently filled with a *p*-type GaN cap layer to form an inverted hexagonal pyramid (Sharma *et al.*, 2000). As for the sidewalls of the inverted

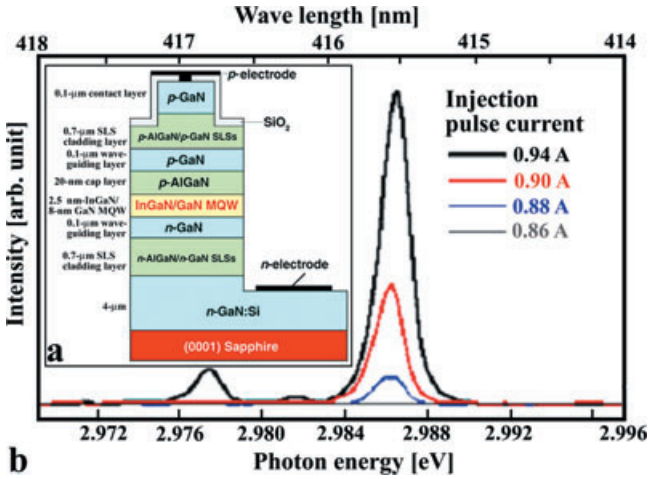

Fig. 1. (a) Structure of a violet laser diode with $In_{0.25}Ga_{0.75}N$ (2.5 nm)/GaN (8nm) MQWs, prepared by metalorganic vapour-phase epitaxy. (b) Room temperature emission spectra of the LD measured under pulsed operation.

hexagonal pyramid on $\{10\bar{1}1\}$ planes, two different structural models were proposed; one is that the sidewalls include thin InGaN/GaN layers (Wu *et al.*, 1998) and the other is that the InGaN QWs end abruptly at the surfaces of the V-pit without thin InGaN/GaN layers (Liliental-Weber *et al.*, 1997; Chen *et al.*, 1998; Sharma *et al.*, 2000). In 1990s, this fundamental issue of the V-defect was unresolved because the atomic-scale structural and compositional analysis was very hard even by conventional analytical high-resolution (HR) transmission electron microscopy (TEM).

We determined the structure of the V-defect using the $In_{0.25}Ga_{0.75}N$ (2.5 nm)/GaN (8 nm) MQWs in a violet LD by means of high-angle annular dark field (HAADF) scanning transmission electron microscopy (STEM) (Watanabe *et al.*, 2003b), and then confirmed it in back-scattering electron images by field-emission scanning electron microscopy (Saijo *et al.*, 2004). They were the first evidential observations of the sidewall MQWs, which supported the model predicted by Wu *et al.* (1998). We revealed the details of this thin six-walled structure with InGaN/GaN $\{10\bar{1}1\}$ layers in the V defects, discussing its formation mechanism (Shiojiri *et al.*, 2006). The specimens used in these experiments were prototype wafers of the violet LD structured as shown in Fig. 1(a), which exhibited a strong emission peak at about 415.5 nm with two small peaks between 416 and 417 nm (Tu *et al.*, 2002). Figure 2(a) reproduces a typical HAADF-STEM image of the $In_{0.25}Ga_{0.75}N$ (2.5 nm)/GaN (8 nm) MQWs that were grown on the *n*-GaN : Si underlying layer and capped with a *p*-AlGaN layer. It was taken with the beam direction parallel to $[\bar{1}2\bar{1}0]$. HAADF-STEM images exhibit strong Z contrast depending on the atomic number, mainly due to incoherent thermal diffuse scattering of electrons. The ten bright stripes parallel to the basal plane are the $In_{0.25}Ga_{0.75}N$ QW layers, whereas the

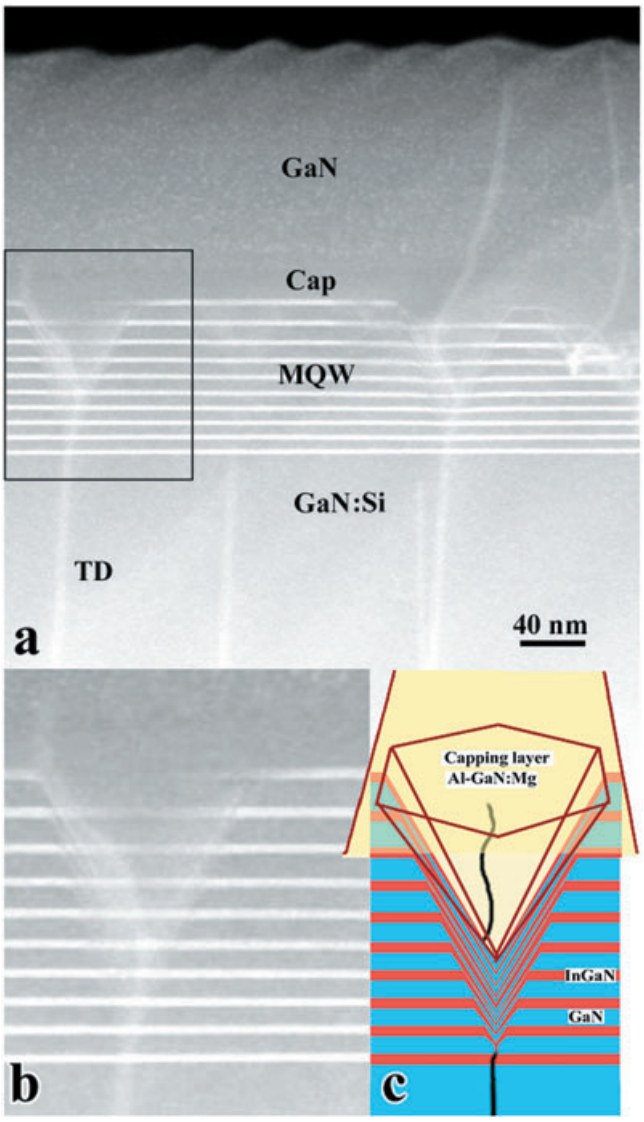

Fig. 2. (a) HAADF-STEM image of a capped $In_{0.25}Ga_{0.75}N$ (2.5 nm)/GaN (8 nm) QW layer grown on the GaN : Si layer, taken in a Tecnai F30, equipped with an objective lens of $Cs = 1.2$ mm, and operated at 300 kV. The HAADF-STEM image was recorded in a detector range of 36–190 mrad, using a convergent electron probe with a semiangle of 26 mrad. (b) Enlarged image of the V defect in the area enclosed by a square in (a). (c) Schematic diagram of the structure of the V defect with the thin six sidewalls of InGaN/GaN $\{10\bar{1}1\}$ layers.

dark stripes are the GaN barrier layers. Both the TDs lying approximately parallel to the *c*-axis and the V defects appear as bright contours. It is clearly seen from Fig. 2(b) that the V defect grew in the form of a thin six-walled structure with thin InGaN/GaN $\{10\bar{1}1\}$ layers and that the TDs propagate to the free surface through the capping layer, as indicated schematically in Fig. 2(c) (Shiojiri *et al.*, 2006). Here, we add that Hangleiter *et al.* (2005) reported on a similar result from a conventional TEM (CTEM) observation. Another example of

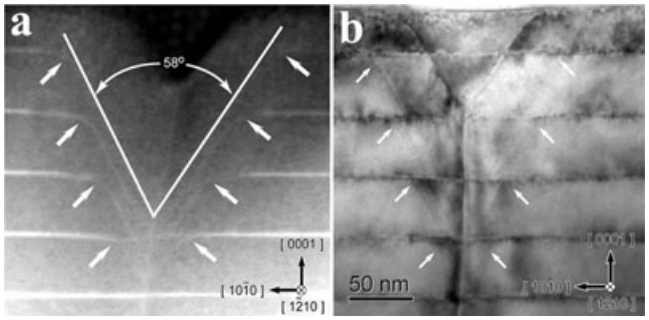

Fig. 3. (a) HAADF-STEM image of a V defect in five 4-nm $In_{0.18}Ga_{0.82}N$ QWs spaced with 40-nm GaN barriers, which were deposited at 800°C on the 2-μm GaN layer and covered with the 50-nm *p*-AlGaN capping layer. (b) CTEM image of the V defect. The apical angle of the V shape nearly agrees with the angle between the $(10\bar{1}1)$ and $(\bar{1}011)$ planes, 56°.

HAADF-STEM image is shown in Fig. 3, together with a CTEM image (Tsai *et al.*, 2007a). The specimen was a prototype wafer of the green emission LD of $In_{0.18}Ga_{0.82}N$ (4 nm)/GaN (40 nm). For the analysis of the structure details, this specimen with the thick QWs and barriers compares favourably with the InGaN (2.5 nm)/GaN (8 nm) MQW shown in Fig. 2. The HAADF-STEM image reveals the structure of the V defect much more definitely than the CTEM image. The CTEM image does not allow us to estimate the thickness of the main QWs (4 nm), to say nothing of thin sidewall InGaN and GaN layers, whereas the HAADF-STEM image does.

We show here a new formation mechanism of the V defects, reviewing the previously proposed mechanisms. Chen *et al.* (1998) assumed that the V defects are initiated by local In segregation in Cottrell atmospheres around the dislocation cores, the In segregation around which inhibits the crystal growth. They showed that Frank's mechanism for the formation of hollow defects (Frank, 1951) is inappropriate for the V defect formation. Wu *et al.* (1998) suggested that the primary cause of the V defect growth is not strain relief, which was premised in Frank's mechanism, but rather the reduced Ga incorporation, which causes the reduction of the growth rate on the $\{10\bar{1}1\}$ planes in comparison with the (0001) plane. Then, we explained the formation of the V defects, taking into account the growth kinetics of the GaN crystal and a masking effect of In atoms by analogy with the epitaxial lateral over-growth (Shiojiri *et al.*, 2006). Hiramatsu *et al.* (1999) showed that in epitaxial lateral over-growth the growth rate of the $\{10\bar{1}1\}$ surfaces of the GaN crystal decreases with decreasing temperature whereas the growth rate of the (0001) surface increases. Therefore, if a mask disturbing the (0001) layer growth is formed at a low reactor temperature, then the growing crystal terminates on the $\{10\bar{1}1\}$ planes, exhibiting the $\{10\bar{1}1\}$ facets. The deposition of the InGaN/GaN MQW layer is usually performed at a temperature as low as 800–850°C because of the low sticking coefficient of In atoms at high temperature. Indium atoms that are trapped and segregated in the strained field (Cottrell atmosphere) around the core of a TD play a role as a small mask, hindering Ga atoms from migrating on the (0001) layer to make a smooth monolayer. A brighter spot and a strong diffraction contour which appear at the apices of the V defects in Fig. 3(a) and (b), respectively, can be considered as the In-rich mask. Once the poor surface diffusion of Ga atoms, and particularly In atoms, impedes the layer-by-layer growth on the (0001) surface with this masking effect, the InGaN and GaN crystals successively grow at the low temperature exhibiting the $\{10\bar{1}1\}$ facets. This results in the six sidewalls of the V-shape pit. Thus, the formation of the V defects is ascribed to the growth at lower temperature. In fact, no V defects occur in the structures such as GaN and AlGaN grown at a temperature as high as 1150°C. We also found that the corners connecting the $\{10\bar{1}1\}$ interfaces on the walls of the V defect with the (0001) interfaces in the main MQWs were curved, as indicated by arrows in Fig. 3 (Tsai *et al.*, 2007a). This was explained as a result of the layer-by-layer growth on the (0001) and $\{10\bar{1}1\}$ surfaces where each monolayer did not cover over its under-monolayer for lack of atom. The successive growth of these monolayers formed an interface with stepwise lattices near the corner, which is observed as the curved corner of the QW in the low-magnified HAADF-STEM images. These curved corners, thus, can be explained by the formation mechanism of V defects.

Light emission and structure of InGaN MQWs

It has been surprised that InGaN-based structures exhibit high emission efficiency despite the great number defect density. Chichibu *et al.* (1996) assigned the electroluminescence peak of the InGaN-based structures to the recombination of excitons localized at certain potential minima in QWs. From cross-sectional TEM and energy dispersive X-ray spectroscopy microanalysis Narukawa *et al.* (1997) showed that the deep localization of excitons (or carriers) originates from the In-rich regions acting as QDs. They noted that the high-quantum efficiency of InGaN-based light emitting diode is mainly due to the large localization of excitons because the pathways of nonradiative recombination are hindered once the excitons are captured in a small volume. Since then several papers have been reported showing the evidence of phase separation in the form of QD structure. Gerthsen *et al.* (2000) and Ruterana *et al.* (2002) indicated In-concentration maps in InGaN layers using strain distribution extracted from HRTEM images, where the linear dependence of the strain on In composition was simply assumed using the Vegard law approximation. Kisielowski *et al.* (1997) presented a similar map obtained by assuming the intensity change in an HRTEM image as the variation of crystal potential in the ultra-thin layer. In any case, these concentration maps were indirectly deduced. An atomically resolved HAADF-STEM image, which provides simultaneously the precise position of the atom columns and the clearly

Z-dependent contrast, allows us to map quantitatively both the strain field and In atom distribution in the InGaN QWs. We thereby mapped the local fluctuation of In atoms in the InGaN layers and directly illustrated the In-rich regions, to be considered as quantum dots, which correspond to the lattice expansion along the *c*-axis (Watanabe *et al.*, 2003a).

Wu *et al.* (1998), who predicted the $\{10\bar{1}1\}$ sidewall QW structure of the V defect, observed the long-wavelength shoulder feature in photoluminescence (PL) and cathodoluminescence correlated with the V defects, and concluded, from the temperature dependence of the cathodoluminescence emission, that the V defect is associated with a localized exciton recombination process. They proposed that either the formation of QD-like structures at the apex of the V defect with each InGaN QW or the luminescence of In-rich pyramid sidewalls is regarded as the source of this long-wavelength shoulder emission. As mentioned in '*Structure and formation mechanism of V defects*' section, we observed the In-rich regions at the apices of the V defects, which were considered as the masks for the V-defect formation (Tsai *et al.*, 2007a). Then, we also concluded that these sidewall InGaN/GN QWs originate additional long-wavelength small emissions like the emissions between 416 and 417 nm in the LD spectrum shown in Fig. 1(b).

Recently, Smeeton *et al.* (2003) have reported that such dot-like structures may be artefacts due to radiation damage during TEM observation because the HRTEM image acquired immediately after first irradiating QW indicated no gross fluctuations of In content in the InGaN alloy. They described that only a brief period of irradiation introduced inhomogeneous strain, which was very similar to that expected from genuine nanometre-scale In composition fluctuations. Then, they expressed there is a possibility of falsely detecting In-rich 'clusters' in a homogeneous QW. Referring this experiment, Hangleiter *et al.* (2005) declared that the unexpectedly high emission efficiency of GaInN-based light emitting diodes relies on self-screening of defects rather than random localization. V-shape pits decorating every TD can be forced to exhibit sidewall QWs with reduced thickness and higher band gap thus leading to a potential barrier around every defect, which keeps carriers from recombining nonradiatively at the defect. They showed that the PL spectra from areas close to defects exhibited, besides the main emission at 430 nm, additional emission peaks in the 380–410 nm range ascribed to the narrow QWs on the $\{10\bar{1}1\}$ sidewalls.

However, the situation seems to have become more confused. Smeeton *et al.* (2003) did not indicate confidently what the damage mechanism is, although they supposed that the localized contrast may be the result of point defect caused by ionization damage of bulk type knock-on displacement of nitrogen (Frenkel pair creation). They touched on nothing about In distribution in the electron beam irradiated QWs. The image recorded within ~20 s shown in the paper by Smeeton *et al.* (2003) exhibited very weak contrast with almost the same feature as that in the image recorded after a few minutes of exposure. The contrast occurred during the expose of 20 s and more may be explained as the In-rich regions in the as-grown InGaN QW, because the strain around the In-rich region would be gradually disclosed if the electron beam irradiation relaxes the lattice in In-rich region forced to have the same spacing with the surroundings. Therefore, the direct composition analysis of the as-grown InGaN QWs should be still necessary to deny either In-rich regions or QDs in the InGaN QWs. The additional short-wavelength emission peaks that Hangleiter *et al.* (2005) observed in PL spectrum would be plausibly ascribed to the thin $\{10\bar{1}1\}$ sidewall QWs. However, Tu *et al.* (2002) did not observe such a short-wavelength emission but observed long-wavelength peaks in the LD emission spectrum. In any case, the observed long-wavelength peaks in LD spectrum (as seen in Fig. 1b) or the long-wavelength shoulder in cathodoluminescence spectrum reported by Wu *et al.* (1998) may not originate without them.

High-density InGaN quantum dots

As mentioned earlier, the In-rich cluster QDs have been proposed to be the origin of the high emission efficiency in the InGaN-based light emitting diodes and LDs (Narukawa *et al.*, 1997). The performance of LDs would be expected to be much improved if the density of QDs be made much higher than that of dislocations. The structures having three-dimensional QDs, instead of QWs in the active layer, have been pursued. One approach for fabricating the three-dimensional InGaN QDs was the deposition of silicon anti-surfactant or SiN_x nanomasks that altered the morphology of the InGaN films from step flow to a three-dimensional island, facilitating the formation of GaN QDs (Tanaka *et al.*, 1996) and InGaN QDs (Hirayama *et al.*, 1998) on the AlGaN. Recently, Tu *et al.* (2004) have prepared an ultra-high density of InGaN QDs of $\sim 3 \times 10^{11}$ cm^{-2} using the SiN_x nanomask. The InGaN QDs exhibited strong PL emission at room temperature. Increasing duration of the SiN_x treatment on the underlying GaN layer provided a red-shift of room temperature–PL peak from violet to green, and broadened the spectrum. Because there were very few structural investigations of the AlGaN QDs besides atomic force microscopy observations, we have examined the ultra-high density InGaN QD devices, using HRTEM, HAADF-STEM and energy dispersive X-ray spectroscopy nanoanalysis (Tsai *et al.*, 2007b). Here we show a similar observation carried out after then.

The sample was prepared by metalorganic vapour phase epitaxy. The structure is schematically shown, together with growth condition, in Fig. 4. Masking with a rough SiN_x layer was formed on the GaN underlying layer, at flow rates of 5 slm for NH_3 and 50 sccm for diluted Si_2H_6. The deposition of a pair of the SiN_x and $In_xGa_{1-x}N$ layers was repeated using a spacer of the GaN : Si barrier layer deposited at 1000°C, and finally the last $In_xGa_{1-x}N$ layer was capped with an undoped GaN layer.

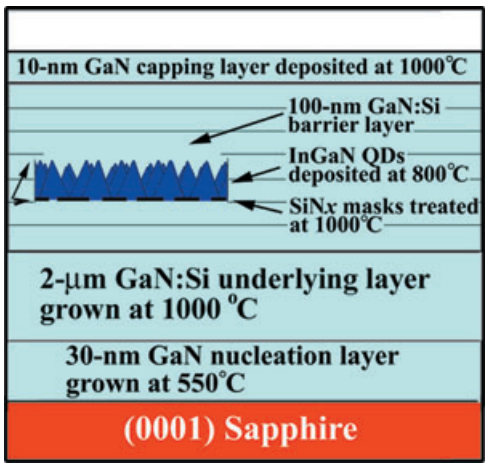

Fig. 4. Structure and growth condition of the sample used in the present experiment.

All the layer thicknesses shown in Fig. 4 are nominal values. The specimens for cross-sectional EM nanoanalysis were prepared by mechanical polishing, followed by ion milling. HAADF-STEM, HRTEM and qualitative energy dispersive X-ray spectroscopy nanoanalysis were performed in a Tecnai F30, equipped with a lens of $Cs = 1.2$ mm, operated at 300 keV. The HAADF-STEM images were recorded in a detector range of $D = 36\sim181$ mrad using a convergent electron probe with a semiangle of $\alpha = 15$ mrad.

Figure 5(a) shows a low-magnified HAADF-STEM image of the specimen. Figure 5(b) is the energy dispersive X-ray spectroscopy spectrum in the area *P*, which comprises emissions from In, Ga, N and Si. Therefore, the bright band around C–D in the HAADF-STEM image might be a layer containing InGaN QDs. From Fig. 5(d), the width of this layer is estimated to be ~15 nm. The intensity profiles of In–L_β along the line C–D (Fig. 5(f)) and also along the line A–B (Fig. 5(d)) indicate that very roughly estimated width of the QDs is 10 nm on the C–D.

Figure 6(a) shows an HAADF-STEM image near the top of the specimen. The dark line is identified as the projection of a layer composed of SiN_x mask islands due to the small thermal diffuse scattering cross-section of Si[14] (and N[7]). The height of the SiN_x masks is roughly estimated to be less than 2 nm from the thickness of the dark line. The InGaN QDs are observed as bright triangles, which look like peaks in a mountain chain, in the HAADF-STEM images (somewhere about between two dotted lines). Figure 6(b) shows an HRTEM image near the specimen edge, where a part of the capping layer was removed during the ion-milling. Quite high QDs (indicated by arrowheads) are seen on the SiN_x mask layer. The SiN_x mask surely has a heavily strained lattice. We could not determine the crystal structure and the composition *x*

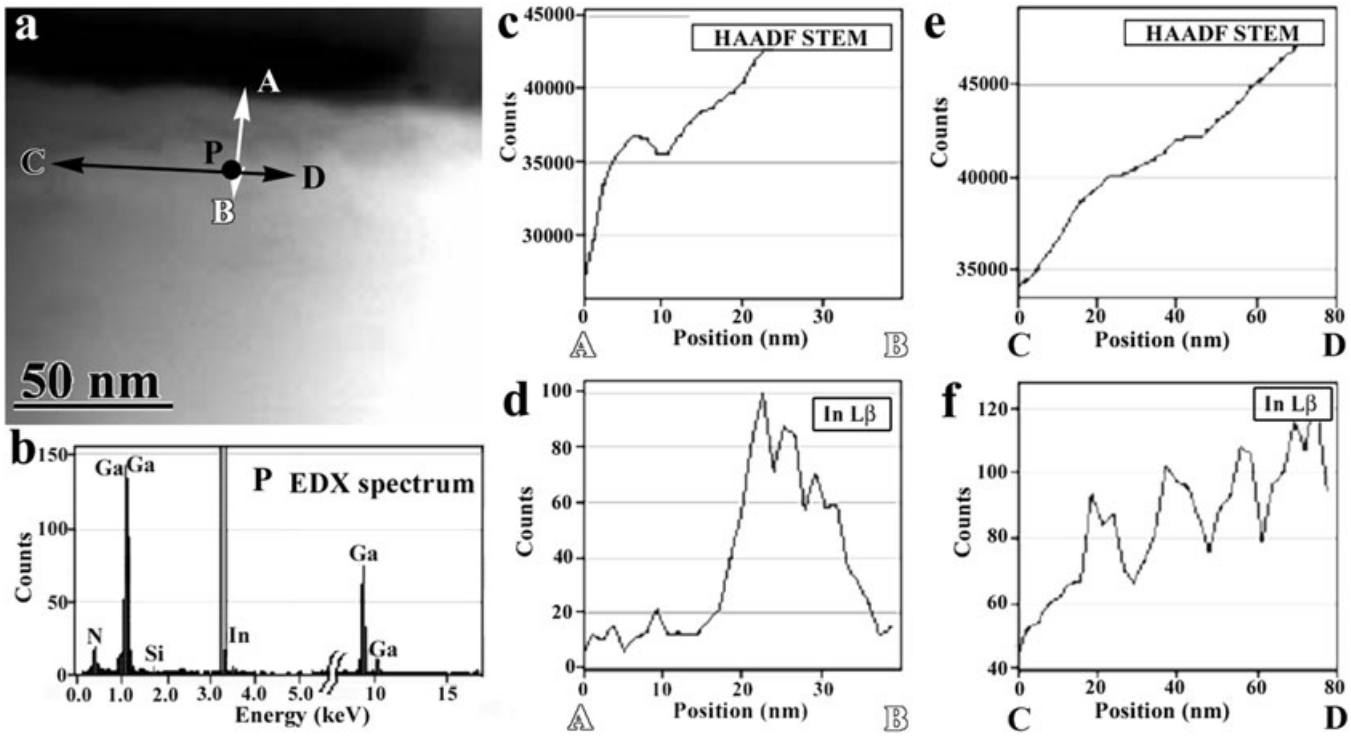

Fig. 5. (a) HAADF-STEM image in which the areas line-scanned for EDX are indicated. (b) Energy dispersive X-ray spectrum in the area *P* (a probe size of ~0.5 nm). (c, d) HAADF-STEM intensity profile and indium L_β intensity profile along the line A–B (~1-nm wide). (e, f) HAADF-STEM intensity profile and indium L_β intensity profile along the line C–D.

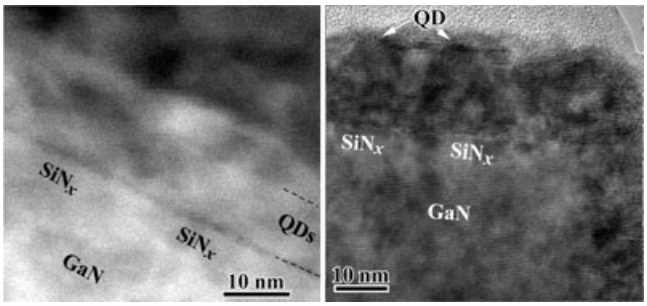

Fig. 6. (a) HAADF-STEM image near the top of the specimen. The layer of SiN_x masks appears as a dark line. The area between two dotted lines comprises the InGaN QDs and is capped with GaN. (b) HRTEM image, where a part of the capping GaN layer was just removed during the ion-milling and InGaN QDs are visible, accordingly.

of the SiN_x. The dark contrast for the QDs may be caused by diffraction effect of the high structure amplitude of In and large lattice strain. The lattices in the InGaN crystals were strained compared with the underlying and the capping GaN lattices, contacting in the coherent lattice relation with them. The QDs can be regarded as nanoisland crystals with the $\{10\bar{1}1\}$ sidewalls and a height of several nanometres (a height as high as 20 nm in this layer). This crystal habit can be understood in taking account of epitaxial lateral over-growth or the crystal growth through masks at lower reactor temperature, as shown in '*Structure and formation mechanism of V defects* section'.

Thus, we can propose the structure for this three-dimensional InGaN quantum dots as the inset in Fig. 4. Further, electrospectroscopic and structural analysis of QDs devices may lead to a solution for whether the high emission efficiency of InGaN-based devices is ascribed to QDs or not.

Acknowledgements

The authors thank Mr. K. Inoke, FEI Company Japan, for taking images in Fig. 2, and Drs. R.C. Tu, C.C. Chuo and T.C. Wang, Industrial Technology Research Institute, Taiwan, and Prof. Z.C. Feng, NTU, for providing the samples.

References

Chen, Y., Takeuchi, T., Amano, H., Akasaki, I., Yamada, N., Kaneko, Y. & Wang, S.Y. (1998) Pit formation in GaInN quantum wells. *Apply. Phys. Lett.* **72**, 710–712.

Chichibu, S., Azuhata, T., Sota, T. & Nakamura, S., (1996) Spontaneous emission of localized excitons in InGaN single and multiquantum well structures. *Appl. Phys. Lett.* **69**, 4188–4190.

Daudin, B., Widmann, F., Feuillet, G., Samson, Y., Arlery, M. & Rouvière, J.L. (1997) Stranski-Krastanov growth mode during the molecular beam epitaxy of highly strained GaN. *Phys. Rev.* **B 56**, R7069–R7072.

Frank, F.C. (1951) Capillary equilibria of dislocated crystals. *Acta Crystallogr.* **4**, 497–501.

Gérard, J.M., Cabrol, O. & Sermage, B. (1996) InAs quantum boxes: highly efficient radiative traps for light emitting devices on Si. *Appl. Phys. Lett.* **68**, 3123–3125.

Gerthsen, D., Hahn, E., Neubauer, B., Rosenauer, A., Schön, O., Heuken, M. & Rizzi, A. (2000) Composition fluctuations in InGaN analyzed by transmission electron microscopy. *Phys. Status Solidi.* **A177**, 145–155.

Hangleiter, A., Hitzel, F., Netzel, C., Fuhrmann, D., Rossow, U., Ade, G. & Hinze, P. (2005) Suppression of nonradiative recombination by V-shaped pits in GaInN/GaN quantum wells produces a large increase in the light emission efficiency. *Phys. Rev. Lett.* **95**, 127402 (4 pages).

Hiramatsu, K., Nishiyama, K., Motogaito, A., Miyake, H., Iyechika, Y. & Maeda, T. (1999) Recent progress in selective area growth and epitaxial lateral overgrowth of III-nitrides: effects of reactor pressure in MOVPE growth. *Phys. Status, Solidi* **A176**, 535–543.

Hirayama, H., Tanaka, S., Ramvall, P. & Aoyagi, Y. (1998) Intense photoluminescence from self-assembling InGaN quantum dots artificially fabricated on AlGaN surfaces. *Appl. Phys. Lett.* **72**, 1736–1738.

Kisielowski, C., Liliental-Weber, Z. & Nakamura, S. (1997) Atomic scale indium distribution in a $GaN/In_{0.43}Ga_{0.57}N/Al_{0.1}Ga_{0.9}N$ quantum well structure. *Jpn. J. Appl. Phys.* **36**, 6932–6936.

Kozodoy, P., Hansen, M., DenBaars, S.P., Mishra, U.K. & Kauffman, J. (1999) Enhanced Mg doping efficiency in $Al_{0.2}Ga_{0.8}N/GaN$ superlattices. *Appl. Phys. Lett.* **74**, 3681–3683.

Liliental-Weber, Z., Chen, Y., Ruvimov, S. & Washburn, J. (1997) Formation mechanism of nanotubes in GaN. *Phys. Rev. Lett.* **79**, 2835–2838.

Nakamura, S., Senoh, M., Nagahara, S., *et al.* (1998) InGaN/GaN /AlGaN based laser diodes with modulation-doped strained-layer superlattices grown on an epitaxially laterally overgrown GaN substrate. *Appl. Phys. Lett.* **72**, 211–213.

Nam, O.H., Bremser, M.D., Zheleva, T. & Davis, R.F. (1997) Lateral epitaxy of low defect density GaN layers via organometallic vapor phase epitaxy. *Appl. Phys. Lett.* **71**, 2638–2640.

Narukawa, Y., Kawakami, Y., Funato, M., Fujita, S., Fujita, S. & Nakamura, S. (1997) Role of self-formed InGaN quantum dots for exciton localization in the purple laser diode emitting at 420 nm. *Appl. Phys. Lett.* **70**, 981–983.

Ruterana, P., Kret, S., Vivet, A., Maciejewski, G. & Dluzewski, P. (2002) Composition fluctuation in InGaN quantum wells made from molecular beam or metalorganic vapor phase epitaxial layers. *J. Appl. Phys.* **91**, 8979–8985.

Saijo, H., Hsu, J.T., Tu, R.C., Yamada, M., Nakagawa, M., Yang, J.R. & Shiojiri, M. (2004) Mapping of multiple quantum wells layers and structure of V-defects in InGaN/GaN diodes. *Appl. Phys. Lett.* **84**, 2271–2273.

Sharma, N., Thomas, P., Tricker, D. & Humphreys, C. (2000) Chemical mapping and formation of V-defects in InGaN multiple quantum wells. *Appl. Phys. Lett.* **77**, 1274–1276.

Shiojiri, M., Chuo, C.C., Hsu, J.T., Yang J.R. & Saijo, H. (2006) Structure and formation mechanism of V-defects in multiple InGaN/GaN quantum wells layer. *J. Appl. Phys.* **99**, 073505 (6 pages).

Smeeton, T.M., Kappers, M.J., Barnard, J.S., Vickers, M.E. & Humphreys, C.J. (2003) Electron-beam-induced strain within InGaN quantum wells: false indium "cluster" detection in the transmission electron microscope. *Appl. Phys. Lett.* **83**, 5419–5421.

Tanaka, S., Iwai, S. & Aoyagi, Y. (1996) Self-assembling GaN quantum dots on $Al_xGa_{1-x}N$ surfaces using a surfactant. *Appl. Phys. Lett.* **69**, 4096–4098.

Tsai, H.L., Wang, T.Y., Yang, J.R., Chuo, C.C., Hsu, J.T., Feng Z.C. & Shiojiri, M. (2007a) Observation of V defects in multiple InGaN/GaN quantum well Layers. *Mater. Trans.* **48**, 894–898.

Tsai, H.L., Yang, J.R., Wang, T.Y., Chuo, C.C., Hsu, J.T. & Shiojiri, M. (2007b) Observation of ultra high density InGaN quantum dots. *J. Appl. Phys.* **102**, 013521 (4 pages).

Tu, R.C., Kuo, W.H., Wang, I.C., Tun, C.J., Hwang, F.C., Chi, J.Y. & Hsu, J.T. (2002) GaN-based violet laser diodes at 415 nm grown by production-scale metalorganic vapor phase epitaxy system. *Proceedings of the 4th International Symposium on Blue Laser and Light Emitting Diode*, pp. 1–4, Cordoba.

Tu, R.C., Tun, C.J., Chuo, C.C., *et al.* (2004) Ultra-high-density InGaN quantum dots grown by metalorganic chemical vapor deposition. *Jpn. J. Appl. Phys.* **43**, L264–L266.

Usui, A., Sunakawa, H., Sasaki, A. & Yamaguchi, A. (1997) Thick GaN epitaxial growth with low dislocation density by hydride vapor phase epitaxy. *Jpn. J. Appl. Phys.* Part 2 **36**, L899–L902.

Watanabe, K., Nakanishi, N., Yamazaki, T., *et al.* (2003a) Atomic-scale strain field and In atom distribution in multiple quantum wells InGaN/GaN. *Appl. Phys. Lett.* **82**, 715–717.

Watanabe, K., Yang, J.R., Huang, S.Y., *et al.* (2003b) Formation and structure of inverted hexagonal pyramid defects in multiple quantum wells InGaN/GaN. *Appl. Phys. Lett.* **82**, 718–720.

Wu, X.H., Elsass, C.R., Abare, A., *et al.* (1998) Structural origin of V-defects and correlation with localized excitonic centers in InGaN/GaN multiple quantum wells. *Appl. Phys. Lett.* **72**, 692–694.

